Journal of Power Sources 195 (2010) 3159–3165

Contents lists available at ScienceDirect

Journal of Power Sources

journal homepage: www.elsevier.com/locate/jpowsour

Effects of crystallization on the high-temperature mechanical properties of a glass sealant for solid oxide fuel cell

Hsiu-Tao Chang[a], Chih-Kuang Lin[a,*], Chien-Kuo Liu[b]

[a] Department of Mechanical Engineering, National Central University, 300 Jhong-Da Rd, Jhong-Li 32001, Taiwan
[b] Nuclear Fuel & Material Division, Institute of Nuclear Energy Research, Lung-Tan 32546, Taiwan

ARTICLE INFO

Article history:
Received 16 November 2009
Received in revised form 1 December 2009
Accepted 1 December 2009
Available online 5 December 2009

Keywords:
Planar solid oxide fuel cell
Glass sealant
Crystallization
High temperature
Mechanical properties

ABSTRACT

Effects of crystallization on the high-temperature mechanical properties of a newly developed silicate-based glass sealant (GC-9) are investigated for use in planar solid oxide fuel cell (pSOFC). The aged, crystallized GC-9 glass is produced by heat treatment of the original GC-9 glass at 900 °C for 3 h. Not only crystalline phases are formed but the residual glass is also changed in the aged GC-9 glass after the heat treatment. Mechanical properties of the aged GC-9 glass are determined by four-point bending technique at temperature from 25 °C to 750 °C. The glass transition temperature of the given glass is reduced but the softening temperature is increased by such a crystallization heat treatment. The aged GC-9 glass exhibits a greater flexural strength and Young's modulus than the non-aged one at temperature below 650 °C due to the existence of crystalline phases. At temperature of 700 °C and 750 °C, a greater extent of stress relaxation is found in the aged GC-9 glass such that its strength and stiffness are much lower than those of the non-aged one. The changes in the thermal and mechanical properties through the given aging treatment are favorable for application of the GC-9 glass sealant in pSOFC.

1. Introduction

Solid oxide fuel cells (SOFCs) offer a potential technology of environment-friendly power generation with high efficiency and fuel flexibility. They are expected to function as standalone power generation units with 5–250 kW [1]. Among the SOFCs developed, the planar SOFC (pSOFC) has lower manufacturing cost and higher power density as compared to the tubular SOFC, but it requires hermetic sealants to maintain gas tight. Due to a high operating temperature of 600–1000 °C, selection of components is a crucial challenge for pSOFC applications. The operating temperature of a pSOFC is restricted by electrochemical reaction that affects the efficiency of cell performance. High operating temperature is an advantage for fuel utilization and for performance of a pSOFC system. On the other hand, disadvantages for cost of materials and long-term stability of components in pSOFC arise. An intermediate operating temperature between 600 °C and 800 °C is a recent trend of development of pSOFC to reduce system cost and enhance long-term stability [2].

A pSOFC stack is a multi-layer structure consisting of repeated units of ceramic anode–electrolyte–cathode assembly and metallic components for a higher voltage. During the stacking process and operation, a suitable sealant used for adherence is needed. Selection of a proper sealant is dependent on stack configuration, assembling condition, and operating temperature. Low leakage, sufficient viscosity, good wetting ability, no chemical reactions with adjacent components, and small thermal expansion mismatch are the important characteristics of a sealant to be used in pSOFC stacks. There are generally two types of seals for pSOFC stacks: compressive seals and rigid seals [3,4]. Compressive seals suffer from problems of oxide scaling and chemical stability in addition to the drawback of an externally applied force [1,3–5]. Rigid seals are therefore more popular than compressive seals [1,3–5]. Among the rigid seals developed, glasses and glass ceramics are the most promising ones to be used in pSOFC systems. However, thermal stress in pSOFC due to mismatch of coefficient of thermal expansion (CTE) and temperature gradient during operation have been recognized as an issue in selecting suitable rigid seals [1,6–9]. Some glass systems rarely crystallize at high temperatures so that they may have an overflow problem. Others may partly or completely crystallize during high-temperature operation. Such crystallized glass seals can offer better physical properties but will cause more serious CTE mismatch [3,10,11]. Crystallization of a glass is sometimes dependent on its composition and thermal events. If a rigid seal is to be used in a pSOFC stack, it must overcome the CTE mismatch issue. Therefore, flowability and crystallization of glass sealants are two important factors related to thermal stress distribution and mechanical integrity in a pSOFC stack. On the other hand, chemical stability of seals is also an important issue. If vaporization of seals

* Corresponding author. Tel.: +886 3 426 7340; fax: +886 3 425 4501.
E-mail address: t330014@cc.ncu.edu.tw (C.-K. Lin).

0378-7753/$ – see front matter © 2009 Elsevier B.V. All rights reserved.
doi:10.1016/j.jpowsour.2009.12.008

occurs during operation, weight loss can lead to sealant collapse [12,13]. A large number of studies on the chemical interactions between sealants and adjacent components and their vaporization reactions in operating atmosphere have been carried out [11–19] and most of them were focused on the chemical stability and compatibility of crystallization process of glasses and glass ceramics in SOFC operating environment. Changes of material properties in the glass sealant due to crystallization might influence its compatibility with other components and the long-term stability and mechanical integrity of a pSOFC stack. Therefore, crystallization of glass sealants during fabrication and cyclic thermal operation is necessary to be investigated. To date, only a few studies [1,10,11] have investigated the complex crystallization effect on the mechanical properties and mechanism behavior of glass sealants.

Different glass systems have been studied for application in various ranges of operating temperature and cell designs of SOFC [3,4]. Recently, a self-healing feature of some glass systems, which have the ability to heal cracks or defects in material at high temperatures, has attracted more attention [1,5,20]. Such seals can meet the long-term operation requirements. A $BaO–B_2O_3–Al_2O_3–SiO_2$ glass (designated as GC-9 glass) recently developed for use in intermediate-temperature (700–750 °C) pSOFC is one kind of these self-healing glass systems [20]. This glass showed good thermal and chemical properties [21–23] and high-temperature mechanical properties [20]. Such a glass system can repair the defects produced during fabrication and/or operation due to a self-healing ability [20]. However, it might crystallize at high temperatures leading to changes of its mechanical properties. There are limited studies [1,10,11] on the effects of crystallization on the mechanical properties of glass sealants for use in pSOFC stacks. This issue is important to design a reliable pSOFC stack and evaluate its long-term structural durability. As part of a series of studies [20] on the high-temperature mechanical properties of glass sealants for pSOFC, the aim of this study is thus to investigate the mechanical properties of the crystallized GC-9 glass and make a comparison with those in its uncrystallized state. In this regard, the crystallization effect on the mechanical properties of such a newly developed glass sealant can be understood. A heat treatment was performed on the GC-9 glass to generate crystalline phases in the material. Systematic four-point bending tests were then conducted at the temperature range of room temperature to 750 °C for the crystallized GC-9 glass (hereafter called aged GC-9 glass) to investigate variation of the mechanical properties with temperature.

2. Experimental procedures

2.1. Glass forming and heat treatment

The chemical composition of the given GC-9 glass includes 0–40 mol% BaO, 0–15 mol% B_2O_3, 0–10 mol% Al_2O_3, 0–40 mol% SiO_2, 0–15 mol% CaO, 0–15 mol% La_2O_3, and 0–5 mol% ZrO_2. It was made by mixing the constituent oxide powders and melting at 1550 °C for 10 h. After melting, it was poured into a mold preheated to 680 °C to produce glass ingots. The glass ingots were then annealed at 680 °C for 8 h and cooled down to room temperature. The crystallization temperatures of the as-cast GC-9 glass were determined as 820 °C and 864 °C [21–23]. In order to study crystallization effect, a crystallization heat treatment was conducted on the as-cast GC-9 glass ingots. The as-cast GC-9 glass ingots were heated from room temperature to 900 °C, held for 3 h, and subsequently cooled down to room temperature. Both the heating rate and cooling rate were set as 5 °C min^{-1}. After such a heat treatment of crystallization, some crystalline phases were formed in the glassy matrix. Such a material state was called aged GC-9 glass to distinguish it from the original, non-aged GC-9 glass.

2.2. Measurement of thermal properties and phase identification

The glass transition temperature (T_g) and softening temperature (T_s) of the original, non-aged GC-9 glass have been determined as 668 °C and 745 °C, respectively [20]. The T_g and T_s of the aged GC-9 glass were determined by thermomechanical analysis (TMA). In this way, T_g and T_s of the aged GC-9 glass were determined as 650 °C and 826 °C, respectively. Crystalline phases of the aged GC-9 glass were determined by X-ray diffraction (XRD) and scanning electron microscopy (SEM) was applied to observe the microstructure and crystalline phases.

2.3. Measurement of mechanical properties

Four-point bending specimens of the aged GC-9 glass were prepared according to ASTM C1211 [24]. The aged glass ingots were cut into rectangular bars with dimensions of 3 mm × 4 mm × 45 mm. In order to prevent the stress concentration effect, the four right-angle corners in the cross-section of each specimen were beveled. Machining direction was along the 45-mm-length longitudinal direction and the tensile surfaces of the specimens were finally polished by 0.3-μm Al_2O_3 powders to minimize the effect of surface defect. Four-point bending tests of the aged GC-9 glass specimens were conducted as per ASTM C1211 [24] to characterize the mechanical properties of this aged glass sealant at operating temperature. The four-point bending tests were performed by using a commercial closed-loop servo-hydraulic testing machine attached with a furnace. The flexural loading fixture with a 20-mm inner loading span and 40-mm outer loading span was made of alumina in order to perform tests at high temperatures. The testing temperatures were set at 25 °C, 550 °C, 600 °C, 650 °C, 700 °C, and 750 °C. For each high-temperature test, the specimen was heated to the specified temperature at a heating rate of 6 °C min^{-1}. The specimen was then held at the specified temperature for 3 min before applying the load. The load was applied under displacement control with a displacement rate of 0.005 mm s^{-1} for all the given testing temperatures. The load–displacement relationship was recorded for each test to calculate the flexural strength and related properties.

2.4. Weibull statistic analysis

The Weibull statistics [25] is widely applied to describe the fracture behavior of brittle materials. Based on a weakest-link hypothesis, it is assumed that the most severe flaw controls the strength. When subjected to an applied stress, σ, the cumulative probability of failure for a brittle material can be expressed by [25]:

$$F = 1 - \exp\left[-\left(\frac{\sigma - \sigma_u}{\sigma_o}\right)^m\right] \quad (1)$$

where F is the failure probability for an applied stress σ, σ_o is a normalizing parameter, σ_u is the threshold stress (below which no failure will occur), and m is the Weibull modulus. Here, the Weibull modulus m is a measure of the degree of strength data dispersion. If σ_u is assumed to be zero, Eq. (1) becomes a two-parameter relation, as shown below [25]:

$$F = 1 - \exp\left[-\left(\frac{\sigma}{\sigma_o}\right)^m\right] \quad (2)$$

This two-parameter Weibull probabilistic equation was applied to analyze the scattering of the strength data generated in the current study. In order to have enough data points for Weibull analysis, more than fifteen specimens were tested at each given testing condition.

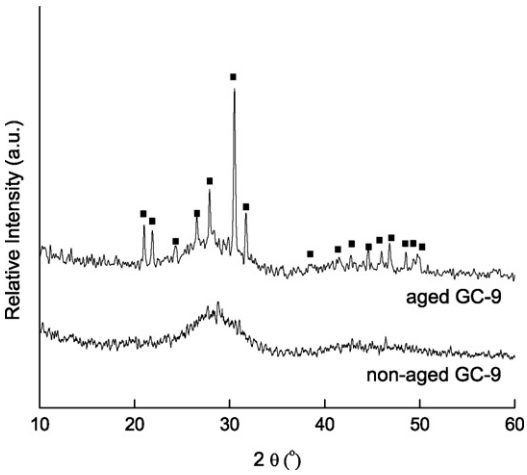

Fig. 1. XRD patterns of non-aged and aged GC-9. The solid squares represent the peaks for $Ba_3La_6(SiO_4)_6$ according to JCPDS No. 27-0038.

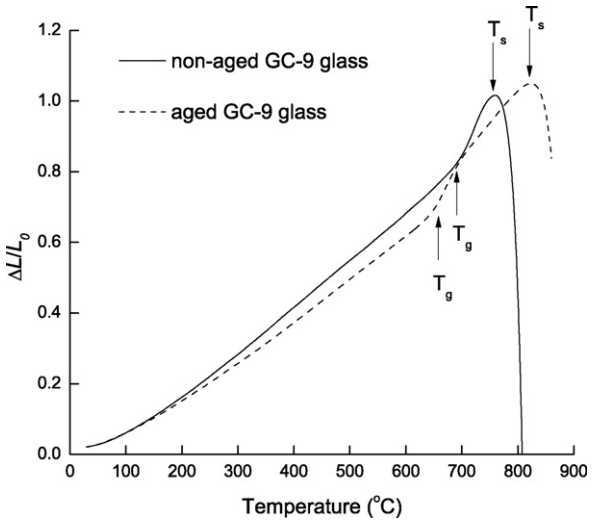

Fig. 3. Thermal expansion curves of non-aged and aged GC-9.

2.5. Determination of Young's modulus

In order to determine the Young's modulus of the given aged glass sealant, equation of an elastic curve for calculating the deflection of a bending beam was applied in the current study. By applying the flexural theory in mechanics of materials [26], a linear force–displacement relationship at the inner loading point can be obtained as follows:

$$E = \frac{a^2(4a - 3L)}{6I} \cdot \frac{P}{v} \quad (3)$$

where E is the Young's modulus, I is the moment of inertia for the beam cross-sectional area, v is the vertical displacement at the inner loading point relative to the outer loading point, P is the half of the applied force, a is the distance between the inner loading point and the outer loading point on the same side, and L is the outer span length. By applying Eq. (3) to the obtained load–displacement data for each tested specimen, the Young's moduli for the aged GC-9 glass at various temperatures were determined.

3. Results and discussion

3.1. Microstructure of aged glass

Crystalline phases of the aged GC-9 glass were characterized by XRD. Fig. 1 shows the XRD patterns for the non-aged and aged GC-9 glass. As shown in Fig. 1, no phase peaks were found in the non-aged GC-9 glass indicating that it is a typically amorphous phase. However, there are several phase peaks present in the curve of the aged GC-9 glass indicating existence of certain crystalline phases in this material. Apparently, holding the GC-9 glass at 900 °C for 3 h indeed induced a certain degree of crystallization in the given glass. The major phase peaks in the XRD pattern of the aged GC-9 glass correspond to a structure of $Ba_3La_6(SiO_4)_6$. Microstructure of the aged GC-9 glass was observed with SEM and shown in Fig. 2. These SEM micrographs showed the existence of crystalline phases embedded in the glassy matrix containing microvoids. The white spots in Fig. 2(b) are the crystalline phases while the residual glass is in the grey region. The crystalline phases are arbitrarily and uniformly distributed in the glassy matrix. The amount of the crystalline phases in the aged GC-9 glass was estimated by calculating the area proportion in several SEM micrographs. As a result, the area proportion of the crystalline $Ba_3La_6(SiO_4)_6$ phase was estimated as 38–41%. This means that the residual glass is the major phase and, presumably, occupies around 60% of the volume in the aged GC-9 glass. The fine and uniform crystalline structure and microvoids throughout the bulk of the aged GC-9 glass are important characteristics. As glass–ceramic materials contain arbitrarily oriented crystals, their properties are independent of orientation. The microvoids observed in the aged GC-9 glass might be generated during glass forming, machining, and/or grinding. They might even be formed during heating or cooling step due to CTE mismatch between the crystalline phases and residual glass of the GC-9 material.

3.2. Thermal properties

Thermal expansion curves of the non-aged and aged GC-9 glass are shown in Fig. 3. CTE mismatch between the non-aged and aged GC-9 glass can be seen in these two curves. Since the thermal expansion curve is an averaged function of each phase in a sample,

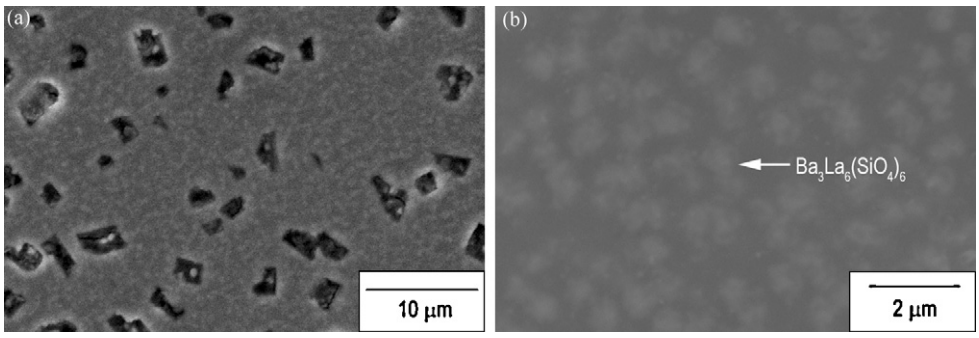

Fig. 2. Microstructure of aged GC-9: (a) overview and (b) high magnification view of crystalline phase.

the difference in these two curves implies that crystallization indeed changed the CTE of the given GC-9 glass. The thermal expansion curve of the non-aged GC-9 glass showed good CTE match with other SOFC component materials [20]. Although the thermal expansion curve of the aged GC-9 glass is different from that of the non-aged state, the CTE of the aged GC-9 glass still has a value in the range of $(9–12)\times10^{-6}\,^{\circ}C^{-1}$. Therefore, the crystallized, aged GC-9 glass is expected to have good CTE match with other SOFC components even though the crystalline phases were generated through aging treatment of the GC-9 glass.

Note the sudden rise in the thermal expansion curve of a typical glass corresponds to the onset of glass transition from solid to liquid state and this point is called T_g. The peak of the thermal expansion curve represents the softening point (T_s). The T_g and T_s of the non-aged and aged GC-9 glass are labeled in Fig. 3. As shown in Fig. 3, the T_g and T_s points of the aged GC-9 glass can be clearly identified indicating existence of residual glass in this aged glass material. Furthermore, the T_g (650 °C) and T_s (826 °C) of the aged GC-9 glass are different from those of the GC-9 glass, 668 °C and 745 °C, respectively. Compared with the non-aged GC-9 glass, the T_g for the aged GC-9 glass is lower while the T_s is greater. It means the residual glass in the aged GC-9 glass was different form the original GC-9 glass and the glass phase was apparently changed during the crystallization process. The chemical composition of the residual glass phase in a glass ceramic is associated with the heat treatment and the initial glass composition [27–29]. The crystallization heat treatment can not only produce crystalline phases but also change the composition of the glass remained in the material. Formation of crystals in the glass can change the CTE of the glass material [30]. In addition, the crystallization can also change the composition of the residual glass such that the T_g and T_s of the material can be changed [30,31]. In this regard, the observed differences in the T_g and T_s between the aged and non-aged GC-9 glass can be attributed to the change of the residual glass in the aged state. Hill and Gilbert [31] studied the variation of T_g with the crystallization and structure changes in a lithium zinc silicate glass through controlled heat treatment. If the network modifier is richer in the crystalline phase, compared to the original glass, then the cross-link density of the residual glass would be expected to increase, and, thereby increasing the T_g [31]. On the other hand, if the network modifier concentration is low in the crystalline phase formed, then the cross-link density of the remaining glass would be decreased such that the T_g is decreased [31]. Accordingly, the decrease of the T_g in the aged GC-9 glass, compared to the non-aged state, might be attributed to the decrease of the cross-link density of network bonds in the residual glass.

3.3. Influence of environmental temperature on mechanical behavior

Typical force–displacement curves for the given non-aged GC-9 glass [20] and aged GC-9 glass under a displacement rate of $0.005\,mm\,s^{-1}$ at 25 °C, 550 °C, 600 °C, 650 °C, 700 °C, and 750 °C are shown in Fig. 4(a) and (b), respectively. The arrows in these figures indicate the specimens were not fractured when the tests were terminated. Three phenomena and two types of mechanical behavior could be observed in the force–displacement curves. Brittle fracture took place at temperature below T_g and stress relaxation occurred above T_g for both the non-aged and aged GC-9 glass. In addition, linear fracture and fracture with a small portion of non-linear deformation was observed when the testing temperature was set below or around T_g, but there was no occurrence of fracture at temperature above T_g. For the non-aged GC-9 glass, brittle and linear fracture could be seen at temperature below T_g (668 °C), i.e. at 25–650 °C. Similar phenomenon also occurred in the aged GC-9 glass at 25–600 °C. Note the T_g for the aged GC-9 glass is 650 °C. However, the aged GC-9 glass exhibited a small portion of non-linear deformation before fracture at 650 °C. As mentioned above, the residual glass was changed during the thermal process such that the T_g of the aged GC-9 glass was shifted to a lower temperature, which is around 650 °C and different from that (668 °C) of the original GC-9 glass. T_g is the temperature point where the glass starts to transform from solid state into liquid state such that the residual glass in the aged GC-9 glass started to influence the mechanical properties when the testing temperature is around its T_g, 650 °C. Glass ceramics usually have a greater stiffness over glasses at high temperature due to the existence of crystalline phase in the matrix [27]. However, there was a different trend in the current study at temperature of 650 °C and above. The main reason is the residual glass has a lower T_g and started to influence the mechanical behavior around its T_g, 650 °C. Note that the volume portion of the residual glass in the aged GC-9 glass is around 60% such that its viscous behavior would play an important role in influencing the mechanical behavior of the aged GC-9 glass at 650 °C and above.

As shown in Fig. 4(a), stress relaxation took place at 700 °C and 750 °C, which are above the T_g of the non-aged GC-9 glass, because of softening of the glass phase. When the testing temperature was at 700 °C and 750 °C, the residual glass in the aged GC-9 glass showed a greater extent of stress relaxation than did the original glass, as shown in Fig. 4(b). This might help release more stress due to thermal mismatch during SOFC operation. T_s is the temperature point where viscosity of a glass reaches a sufficiently low value such that the glass can not support its shape under its own weight. The T_s of

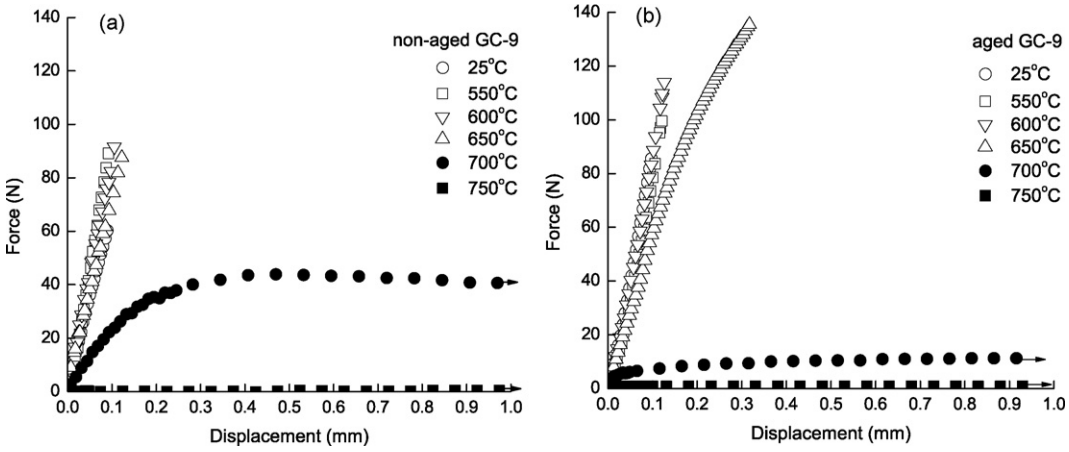

Fig. 4. Typical force–displacement relationship under a displacement rate of $0.005\,mm\,s^{-1}$ at various temperatures: (a) non-aged GC-9 and (b) aged GC-9.

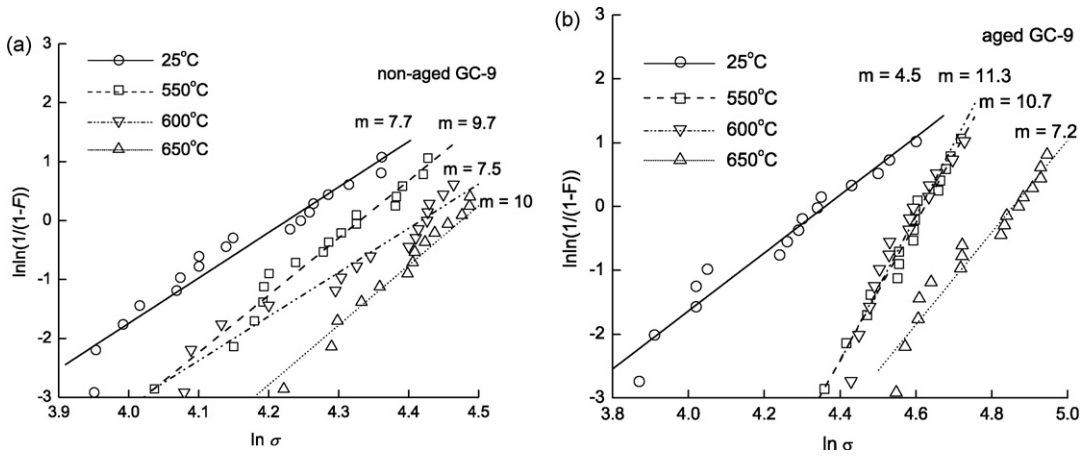

Fig. 5. Weibull distribution of flexural strength: (a) non-aged GC-9 and (b) aged GC-9 (the unit of σ is MPa).

the aged GC-9 glass was shifted to a temperature higher than that of the original GC-9 glass, from 745 °C to 826 °C. Because of such an increase of T_s, it is expected that the aged GC-9 glass sealant would not flow out at the targeted working temperature of an intermediate-temperature pSOFC. In this regard, the sealing function of the aged GC-9 glass can still be maintained at 700–750 °C even though a greater extent of deformation and stress relaxation would take place. From this point of view, control of the crystalline phase and residual glass is important to develop a suitable sealant for pSOFC.

In the present study, not only fracture with a small portion of non-linear deformation but also a greater extent of stress relaxation for the aged GC-9 glass could be seen at temperature higher than T_g. The residual glass in the aged GC-9 glass was the main factor to control the high-temperature mechanical behavior at temperature of 650 °C and above even though the crystalline phases were present in the aged GC-9 glass. Nguyen et al. [32] attributed the non-linear response of a G-18 glass at high temperature to viscoelastic behavior of porous and glassy phases, void initiation and growth, crystalline/glass phase decohesion, microcracking and/or plasticity of glassy phases. In the current study, although the aged GC-9 glass was crystallized during heat treatment, non-linear response still took place at 650 °C and above. Such a non-linear response was considered to be caused by viscoelastic and/or plastic flow of the glassy phase at temperature of T_g or above for the aged GC-9 glass. The T_g of the aged GC-9 glass was shifted to 650 °C and, therefore, the non-linear response occurred at a lower temperature than that in the non-aged GC-9 glass. As the expected working temperature for the given aged GC-9 glass is between 700 °C and 750 °C, the stress relaxation phenomenon is favorable in reducing the stresses produced from thermal mismatch.

3.4. Fracture strength and Weibull statistics

For a progress toward a more reliable sealant, the Weibull statistics was applied to analyze the experimental data. The two-parameter Weibull distribution (Eq. (2)) of flexural strength for the non-aged [20] and aged GC-9 glass at different temperatures is shown in Fig. 5. Table 1 lists the mean values of the flexural strength and Weibull modulus, m, for the given non-aged and aged GC-9 glass at various temperatures. The data for 700 °C and 750 °C are not the fracture strength but the mean values of the maximum flexural stress applied during test. Similar to the previous results of the non-aged GC-9 glass [20], the flexural strength of the aged GC-9 glass was also increased with temperature for a given failure probability from room temperature to 650 °C. Note that the fracture strength of the aged GC-9 glass at 550 °C and 600 °C can be seen as comparable, as the data points of these two temperatures are merged together. Such an increase of flexural strength with temperature at temperature below the T_g of the non-aged GC-9 glass resulted from a crack healing effect [20]. This self-healing effect could repair cracks or defects at high temperatures and enhance the mechanical properties of a glass or glass ceramic. Apparently, a similar self-healing mechanism was present in the residual glass of the aged GC-9 glass leading to the increase of flexural strength with temperature from 25 °C to 650 °C.

The flexural strength of the aged GC-9 glass at temperature from room temperature to 650 °C is greater than that of the non-aged GC-9 glass, as shown in Fig. 5 and Table 1. Mechanical properties of glass–ceramic materials generally depend on the mechanical properties of the main crystalline phases, which occupy a portion of the volume in material [27]. In the current work, when the testing temperature was below the T_g, such as room temperature to 650 °C, the crystalline phase indeed enhanced the flexural strength of the aged

Table 1
Mean value of flexural strength and Weibull modulus for non-aged and aged GC-9 glass at various temperatures.

Material	Temperature					
	25 °C	550 °C	600 °C	650 °C	700 °C	750 °C
Flexural strength (MPa)						
Non-aged GC-9 glass	63	73	82	83	40[a]	4.5[a]
Aged GC-9 glass	73	95	98	112	7.7[a]	0.1[a]
Weibull modulus						
Non-aged GC-9 glass	7.7	9.7	7.5	10	–	–
Aged GC-9 glass	4.5	10.7	11.3	7.2	–	–

[a] Maximum flexural stress applied during test.

Table 2
The average values of Young's modulus and standard deviation for non-aged and aged GC-9 glass at various temperatures.

Material	Temperature				
	25 °C	550 °C	600 °C	650 °C	700 °C
Young's modulus (GPa)					
Non-aged GC-9 glass	66 (7.9)	66 (8.3)	64 (6.8)	59 (5.4)	17 (7.0)
Aged GC-9 glass	68 (6.3)	71 (9.6)	72 (4.3)	47 (12)	2.6 (1.6)

GC-9 glass, as compared to the non-aged one. However, when the testing temperature was around or greater than T_g, such as 650 °C, 700 °C, and 750 °C, the viscous characteristics of the residual glass in the aged GC-9 glass played a very important role to reduce the load-carrying ability of the given aged glass. As described above, the residual glass in the aged GC-9 glass was different from the original GC-9 glass. As shown in Table 1, the load-carrying ability of the residual glass in the aged GC-9 glass at 700 °C and 750 °C was inferior to that of the original GC-9 glass.

The values of the Weibull modulus at 550 °C, 600 °C, and 650 °C are greater than that at room temperature for both the non-aged and aged GC-9 glass. A large Weibull modulus represents a less degree of scattering in strength data, which was caused by a smaller range of distribution in flaw size and shape. It has been confirmed that outlines of the defects on the surfaces of the non-aged GC-9 glass specimens at high temperature could be modified or healed due to the aforementioned crack healing effect [20]. This self-healing effect presumably also took place in the aged GC-9 glass. As the crack healing mechanism could relax the stress concentration around surface flaws, change flaw outlines or totally heal the crack, scattering of the strength data at high temperature became smaller [20]. Note the improvements of the Weibull modulus at high temperatures over room temperature for the aged GC-9 glass were greater than those for the non-aged GC-9 glass. This implies that there was a superior crack healing effect acting on the aged GC-9 glass from the residual glass in the aged GC-9 glass. The Weibull modulus of the aged GC-9 glass at room temperature was smaller than that of the non-aged GC-9 glass, while the values at high temperatures were greater than those of the non-aged GC-9 glass except at 650 °C. It is obvious that the strength-determining defects at room temperature were different from those at high temperatures. There are crystalline phases and microvoids in the aged GC-9 glass (Fig. 2(a)) so that the scattering of the strength data at room temperature was greater than that of the non-aged GC-9 glass without any crystalline phase. However, the scattering of the strength data of the aged GC-9 glass at 550 °C and 600 °C was smaller than that of the non-aged one as the residual glass in the aged GC-9 glass more effectively healed the defects in the matrix. Apparently, the residual glass in the aged GC-9 glass had a better flowable ability than did the glassy phase of the non-aged GC-9 glass. However, the aged GC-9 glass at 650 °C shows a reduction of the Weibull modulus, possibly, due to a competition of deformation mechanism between brittle fracture and viscous flow at temperature around T_g.

3.5. Influence of environmental temperature on Young's modulus

Table 2 lists the calculated Young's moduli (averaged value and standard deviation) at various temperatures for the non-aged and aged GC-9 glass. As there was significant stress relaxation at 750 °C for both the non-aged and aged GC-9 glass, their Young's modulus could not be determined at this temperature. The Young's modulus of the non-aged and aged GC-9 glass barely changed with temperature form room temperature to 600 °C, as shown in Table 2. Note that the averaged value of the Young's modulus for the aged GC-9 glass is slightly larger than the corresponding one of the non-aged GC-9 glass at the temperature range of 25–600 °C due to absence of crystalline phase in the non-aged one. Above 600 °C, the Young's modulus for both the non-aged and aged GC-9 glass exhibited a decrease with an increase in temperature and the Young's modulus of the aged GC-9 glass even showed a lower value than that of the non-aged one. The non-aged and aged GC-9 glass behaved as a brittle material at temperature below T_g so each of their Young's modulus remained comparable from room temperature to 600 °C. These results are different from the variation of Young's modulus with temperature for a glass sealant which was measured by a dynamic resonance technique [11]. Liu et al. [11] measured the Young's modulus of the non-aged and aged G-18 glass at temperature from room temperature to 800 °C. The Young's modulus of the aged G-18 glass increased with temperature at temperatures below 400 °C, exhibited a temperature-independent manner from 400 °C to 600 °C, and started to decrease with increasing temperature from 600 °C to 800 °C [11]. However, in the present work, the aged GC-9 glass did not show an increase of Young's modulus with temperature at low temperatures. When the testing temperature was around or above T_g, the Young's modulus of the aged GC-9 glass was temperature dependent due to a lot of residual glass present in the material. For the aged GC-9 glass, the residual glass phase at temperature around and above T_g became viscous and played an important role in influencing the mechanical properties of this material. Due to such viscous behavior of the residual glass, the aged GC-9 glass at temperature around and above T_g started to lose its structure stiffness and even showed a lower Young's modulus than that of the non-aged GC-9 glass at 650 °C and 700 °C. Again, it is evidenced that the residual glass in the aged GC-9 glass was different from the glass phase of the non-aged GC-9 glass.

4. Conclusions

Crystalline phases ($Ba_3La_6(SiO_4)_6$) were formed in the aged GC-9 glass by a heat treatment at 900 °C for 3 h and the residual glass in the aged GC-9 glass was also changed. Through such a heat treatment, the T_g of the aged GC-9 glass sealant was reduced from 668 °C to 650 °C while the T_s was increased from 745 °C to 826 °C. Apparently, the residual glass in the aged GC-9 glass was different from the original GC-9 glass in terms of such variation in thermal properties.

T_g and T_s are the two important temperature indices for the high-temperature mechanical properties of the non-aged and aged GC-9 glass. Both materials exhibited an increase of flexural strength with temperature at temperature below their own T_g due to a crack healing effect. At temperature above T_g, the flexural strength and Young's modulus of both the non-aged and aged GC-9 glass were significantly reduced due to viscous characteristic of the glass phases.

At temperature below 650 °C, the flexural strength and structural stiffness of the aged GC-9 glass were enhanced by formation of crystalline phases in the glass matrix, as compared to the non-aged, original GC-9 glass. However, when the testing temperature was increased to 700 °C and 750 °C, the flexural strength and Young's modulus of the aged GC-9 glass was significantly lower than those of the non-aged one due to a greater extent of stress relaxation provided by the residual glass phase in the aged GC-9 glass.

The given crystallization heat treatment is favorable for applying the GC-9 glass sealant to intermediate-temperature pSOFC, as

crystalline phases in the aged GC-9 glass can offer a greater strength at low temperature and the residual glass can offer a greater effect on releasing the stress generated by thermal mismatch during SOFC operation.

Acknowledgement

This work was supported by the National Science Council (Taiwan) under Contract No. NSC 95-2221-E-008-004-MY3.

References

[1] N. Govindaraju, W.N. Liu, X. Sun, P. Singh, R.N. Singh, J. Power Sources 190 (2009) 476–484.
[2] A. Weber, E. Ivers-Tiffée, J. Power Sources 127 (2004) 273–283.
[3] J.W. Fergus, J. Power Sources 147 (2005) 46–57.
[4] P.A. Lessing, J. Mater. Sci. 42 (2007) 3465–3476.
[5] R.N. Singh, Int. J. Appl. Ceram. Technol. 4 (2007) 134–144.
[6] C.S. Montross, H. Yokokawa, M. Dokiya, Br. Ceram. Trans. 101 (2002) 85–93.
[7] A. Atkinson, B. Sun, Mater. Sci. Technol. 23 (2007) 1135–1143.
[8] C.-K. Lin, T.-T. Chen, Y.-P. Chyou, L.-K. Chiang, J. Power Sources 164 (2007) 238–251.
[9] C.-K. Lin, L.-H. Huang, L.-K. Chiang, Y.-P. Chyou, J. Power Sources 192 (2009) 515–524.
[10] K.D. Meinhardt, D.-S. Kim, Y.-S. Chou, K.S. Weil, J. Power Sources 182 (2008) 188–196.
[11] W. Liu, X. Sun, M.A. Khaleel, J. Power Sources 185 (2008) 1193–1200.
[12] K. Eichler, G. Solow, P. Otschik, W. Schaffrath, J. Eur. Ceram. Soc. 19 (1999) 1101–1104.
[13] T. Jin, K. Lu, J. Power Sources 195 (2010) 195–203.
[14] N. Lahl, K. Singh, L. Singheiser, K. Hilpert, D. Bahadur, J. Mater. Sci. 35 (2000) 3089–3096.
[15] Z. Yang, K.D. Meinhardt, J.W. Stevenson, J. Electrochem. Soc. 150 (2003) A1095–A1101.
[16] S.-B. Sohn, S.-Y. Choi, G.-H. Kim, H.-S. Song, G.-D. Kim, J. Am. Ceram. Soc. 87 (2004) 254–260.
[17] Y.-S. Chou, J.W. Stevenson, R.N. Gow, J. Power Sources 168 (2007) 426–433.
[18] Y.-S. Chou, J.W. Stevenson, R.N. Gow, J. Power Sources 170 (2007) 395–400.
[19] F. Smeacetto, M. Salvo, M. Ferraris, J. Cho, A.R. Boccaccini, J. Eur. Ceram. Soc. 28 (2008) 61–68.
[20] H.-T. Chang, C.-K. Lin, C.-K. Liu, J. Power Sources 189 (2009) 1093–1099.
[21] C.-K. Liu, T.-Y. Yung, K.-F. Lin, Proceedings of the Annual Conference of the Chinese Ceramic Society 2007 (CD-ROM), 2007 (in Chinese).
[22] C.-K. Liu, T.-Y. Yung, S.-H. Wu, K.-F. Lin, Proceedings of the MRS_Taiwan Annual Meeting 2007 (CD-ROM), 2007 (in Chinese).
[23] C.-K. Liu, T.-Y. Yung, K.-F. Lin, Proceedings of the Annual Conference of the Chinese Ceramic Society 2008 (CD-ROM), 2008 (in Chinese).
[24] ASTM Standard C1211, Standard Test Method for Flexural Strength of Advanced Ceramics at Elevated Temperature, Annual Book of ASTM Standards, vol. 15.01, ASTM International, West Conshohocken, PA, USA, 2005, pp. 268–284.
[25] D.W. Richerson, Modern Ceramic Engineering, 2nd ed., Marcel Dekker, Inc., New York, USA, 1992.
[26] R.C. Hibbeler, Statics and Mechanics of Materials, SI ed., Prentice Hall, Inc., Singapore, 2004.
[27] Z. Strnad, Glass–Ceramic Materials, Elsevier Science Publishing Company, Inc., New York, USA, 1986.
[28] D.G. Burnett, R.W. Douglas, Discuss. Faraday Soc. 50 (1970) 200–205.
[29] D.G. Burnett, R.W. Douglas, Phys. Chem. Glasses 12 (1971) 117–124.
[30] J.E. Shelby, Introduction to Glass Science and Technology, 2nd ed., The Royal Society of Chemistry, New York, USA, 2005.
[31] R. Hill, P. Gilbert, J. Am. Ceram. Soc. 76 (1993) 417–425.
[32] B.N. Nguyen, B.J. Koeppel, S. Ahzi, M.A. Khaleel, P. Singh, J. Am. Ceram. Soc. 89 (2006) 1358–1368.